The 1997 periastron passage of the binary pulsar PSR B1259-63

S. Johnston¹, N. Wex^{2,1}, L. Nicastro³, R. N. Manchester⁴ & A. G. Lyne⁵

- ¹Research Centre for Theoretical Astrophysics, University of Sydney, NSW 2006, Australia
- ² Max-Planck-Institut für Radioastronomie, Auf dem Hügel 69, D-53121 Bonn, Germany
- ³ Istituto di Fisica Cosmica con Applicazioni all'Informatica, CNR, Via U. La Malfa 153, I-90146 Palermo, Italy
- ⁴ Australia Telescope National Facility, CSIRO, PO Box 76, Epping, NSW 2121, Australia
- ⁵ University of Manchester, Jodrell Bank Observatory, Macclesfield, Cheshire SK11 9DL, UK

24 October 2018

ABSTRACT

We report here on multifrequency radio observations of the pulsed emission from PSR B1259–63 around the time of the closest approach to its B2e companion star. There was a general increase in the pulsar's dispersion measure and scatter broadening, and a decrease in the flux density towards periastron although changes in these parameters were seen on timescales as short as minutes. The pulsed emission disappeared 16 days prior to periastron and remained undetectable until 16 days after periastron.

The observations are used to determine the parameters of the wind from the Be star. We show that a simple model, in which the wind density varies with radius as r^{-2} , provides a good fit to the data. The wind is clumpy with size scales $\leq 10^{10}$ cm, densities of $\sim 10^6$ cm⁻³ and a velocity of ~ 2000 km s⁻¹ at a distance of 20 - 50 stellar radii. We find a correlation between dispersion measure variations and the pulse scattering times, suggesting that the same electrons are responsible for both effects.

Key words:

binary pulsars – pulsars: individual (PSR B1259–63)

1 INTRODUCTION

The pulsar PSR B1259-63 is a member of a unique binary system. Discovered using the Parkes telescope in a survey of the Galactic plane at 1.5 GHz (Johnston et al. 1992a), it was shown by Johnston et al. (1992b) to be in a highly eccentric 3.4-yr orbit with a 10th-magnitude Be star, SS 2883.

Extensive observations of this system have been made, particularly near the previous periastron passage on 1994 January 9. These include observations at radio wavelengths (Johnston et al. 1996; McClure-Griffiths et al. 1998; Wex et al. 1998; Johnston et al. 1999), optical (Johnston et al. 1994), in the X–ray (Cominsky, Roberts & Johnston 1994; Kaspi et al. 1995; Hirayama et al. 1996) and in γ -rays (Grove et al. 1995; Hirayama et al. 1999). These observations have led to a better understanding of the physical conditions in the wind and disc of the Be star (Tavani, Arons & Kaspi 1994; King & Cominsky 1994; Melatos, Johnston & Melrose 1995; Tavani & Arons 1997; Johnston et al. 1999; Ball et al. 1999).

The understanding of the system is thus as follows: SS 2883 is a (main-sequence) B2e star with mass ${\sim}10~M_{\odot}$ and radius ${\sim}6~R_{\odot}$. Its characteristic emission disc extends to at least 20 R_* in the optical, similar to the distance between the pulsar and Be star at periastron. It is likely that the disc

is highly tilted with respect to the orbital plane; the orbital plane is itself at 36° with respect to the line of sight. Due to the misalignment of the emission disc with the orbital plane, the pulsar goes behind the disc (with respect to the observer) near \mathcal{T} –16 and emerges from the front of the disc near \mathcal{T} +14. (Here, \mathcal{T} is the epoch of periastron). The disc material is extremely dense near the stellar surface but falls off rapidly as a function of distance. The polar wind, by contrast is $\sim 10^4$ times less dense than the disc material at the stellar surface and has an r^{-2} density profile.

The radio observations of the pulsed emission from the 1994 periastron were rather crude in the sense that frequency agility was limited, with frequency switching requiring manual receiver changes and hence only possible on a \sim 1 day timescale. Furthermore, only relatively few observations were obtained before and after the eclipse of the pulsar. In 1994 there was no real-time pulse folding software which limited our best observing strategy in that the off-line data reduction significantly lagged behind the observing. However, these observations showed dispersion measure (DM) and scintillation parameter changes on timescales of at least as short as one day and demonstrated that these changes were highly asymmetric with respect to periastron (Johnston et al. 1996).

In this paper we report on observations of the pulsed radio emission made around the latest periastron passage of the pulsar on 1997 May 29. Section 2 describes the observations. In Section 3 we present the results and in Section 4 discuss their implications.

OBSERVATIONS

In 1996, a major upgrade was made to the focus cabin of the Parkes radio-telescope which allowed several receivers to be placed on a movable platform. This enables the choice of receiver to be made from the control room and allows for frequency changes in only a few minutes.

We observed PSR B1259-63 regularly with the 64-m Parkes radio telescope at frequencies of 1.4, 4.8 and 8.4 GHz (Wex et al. 1998). The observations were intensified around the periastron passage of the pulsar on 1997 May 29. At each frequency the receiver consists of a dual-channel, cryogenically cooled system sensitive to two orthogonal linear polarizations.

Data were recorded simultaneously using two recording systems. The Caltech Fast Pulsar Timing Machine (FPTM) is a correlator capable of fast sampling (Navarro 1994). The signals from the two polarizations are down-converted to intermediate frequency and 2-bit digitised by the FPTM which computes correlation functions (CFs) with 128 lags over a 128 MHz bandwidth. The system can be used either to record full Stokes parameters for one 128 MHz bandwidth or total intensity for two independent bandwidths. For the higher frequencies we always recorded the data in full Stokes mode, with the band centered at 4800.25 and 8400.25 MHz. In the 20cm band, we either recorded the full Stokes parameters at 1351.0 MHz or two independent bandwidths centered at 1274.75 and 1396.0 MHz. The CFs are then hardware integrated at the apparent pulsar period (\sim 47 ms) and the data recorded every 60 s. A graphical output displays the pulse profile every integration cycle. Thus, changes in observing strategy could be made in real-time.

Simultaneously, we also recorded data using a filterbank detection system in an identical fashion to that described elsewhere (e.g. Johnston et al. 1996). The signals from the receivers were down-converted to an intermediate frequency and then passed into a filterbank which consisted of 64 channels, each 5 MHz wide for a total of 320 MHz. Full Stokes parameters were recorded every 0.6 ms and written to magnetic tape for off-line analysis. The centre frequencies were 1374, 4748 and 8348 MHz.

For flux density calibration, observations were made of Hydra A at 1.4, 4.8 and 8.4 GHz once every few days at the telescope. These measurements yielded system flux densities of ~ 28 , ~ 100 and ~ 100 Jy at the three frequencies. Before every observation of the pulsar, a pulsed noise source, injected at 45 degrees to the signal probes, was recorded. This allows for calibration of the system gains and phases.

Derivation of the Dispersion Measure

Over a period of a few hours we obtained observations at 5 different frequencies: 1.2, 1.4, 1.5, 4.8 and 8.4 GHz. The three frequencies in the 20-cm band were obtained simultaneously. The observation would then be followed by one at either 4.8 and 8.4 GHz before again observing the 20cm band. Typical observations were 1-hr in duration. Pulse time-of-arrivals were obtained in the standard manner (e.g. Wex et al. 1998). The DM was obtained by assuming the DM contribution from the 1.5 kpc path through the interstellar medium is 147.6 cm⁻³pc and does not change with time. Then, the extra DM contribution from the wind of the Be star could be computed by the relative differences in the residuals between the different frequencies. Having closely spaced frequencies in the 20-cm band allows any ambiguities to be resolved (i.e. where the ΔDM could impose more than 1 phase turn on the residual). Typical errors using this method are small ($\sim 0.1 \text{ cm}^{-3}\text{pc}$), much smaller than those obtained simply from fitting the delays in frequency-phase space over a single observing band.

Derivation of the Scattering Time

Scatter-broadening of a pulse can be approximated by convolving the intrinsic pulse shape with a truncated exponential function. The situation for PSR B1259-63 is somewhat complicated by the presence of two strong pulses, only 20 ms apart in time (Manchester & Johnston 1995). For large scattering times, the scatter tail of the first pulse overlaps the second pulse and this must be taken into account in the derivation of the scattering time. We used the Levenberg-Marquart method (LMM) to perform a least-squares fit to the observed profile given a 'standard' (unscattered) profile. The fit returns the 4 free parameters: amplitude, baseline and decay time of the exponential and the offset in time between the profiles. Generally, for scattering times less than 7 ms, the fits are good. Above this, however, the pulses tend to be weak, and the extremely scattered and weak pulses make the fitting less robust. This is reflected in much larger errors bars on the fitted parameters.

RESULTS

The broad overview of the observational data is as follows. A change in the DM over and above that from the ISM was first observed at \mathcal{T} -48. Over a period of \sim 20 days, both the DM and the pulse scattering showed an overall increase, and strong hourly variations. The pulsed emission was last detected on \mathcal{T} -17. Observations made on \mathcal{T} –15 showed no pulsed emission at any frequency, a result confirmed with independent observations on the Australian Telescope Compact Array (Johnston et al. 1999). The pulses were re-detected at Parkes on \mathcal{T} +16, following a non-detection two days earlier. Post-periastron, no change in DM or pulse-scattering could be measured, although significant changes in rotation measure and polarization properties were recorded. Significant flux variability was seen both prior to and following the eclipse. The general trend though was towards lower fluxes in the few days before and after the eclipse.

Figure 1 shows the DM changes and the scattering time, τ , as a function of epoch prior to periastron. Figure 2 shows a shorter time span of only 8 days prior to the eclipse.

The figures show a wealth of detail. Points to note are that the DM changes on short timescales (~ 1 hr or less) by $\sim 1 \text{ cm}^{-3}\text{pc}$. There is a slow increase in the DM from \mathcal{T} -50

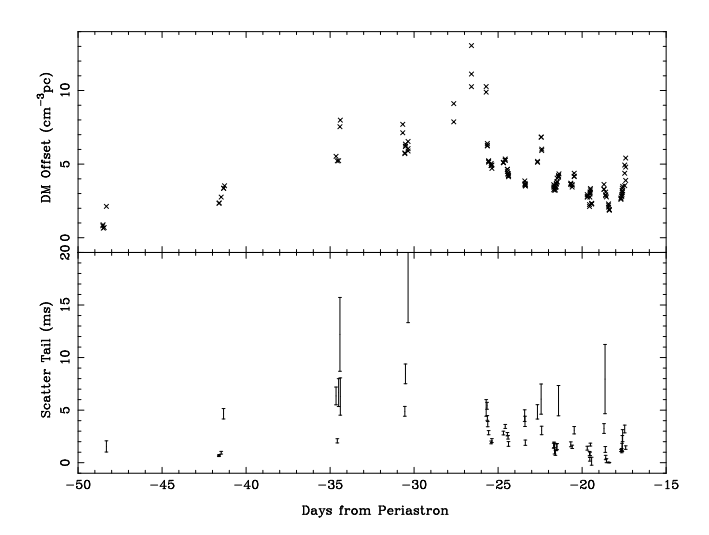


Figure 1. Dispersion Measure changes and derived scattering times as a function of time prior to periastron. The errors on the DM are of order 0.1 cm⁻³pc and are too small to be seen on the plot.

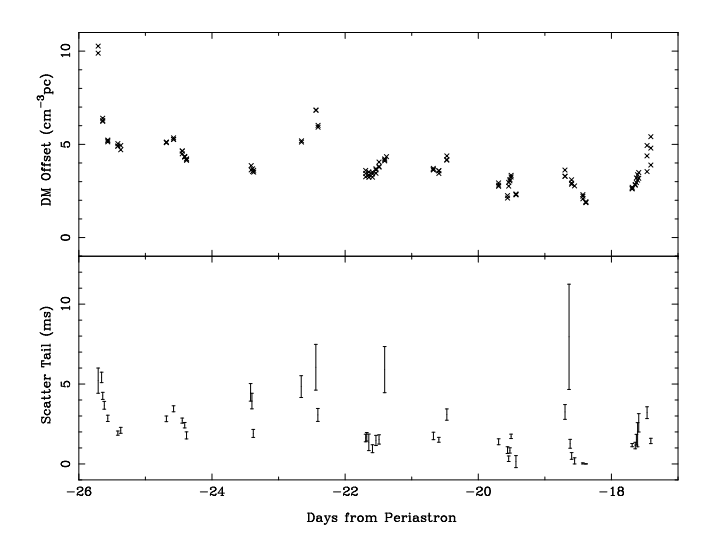


Figure 2. As Fig. 1, showing a period of only 8 days just prior to the eclipse of the pulsar.

until -27. The DM then slowly drops, before rising steeply again at \mathcal{T} -17. The pulsar was undetected following these observations until \mathcal{T} +16. Both the daily variations and the drop in DM towards \mathcal{T} -20 are evidence for the clumpy nature of the wind.

Flux density variations in PSR B1259–63 occur on a number of timescales. The diffractive scintillation timescale at GHz frequencies close to periastron is expected to be very short ($\ll 1$ second) and hence unobservable. The refractive timescale is probably of the order of minutes. One also expects changes in the flux density due to free-free absorption as the pulsar moves behind clumps in the Be star wind. In Figure 3, we show flux variations as a function of time starting on 1997 May 8.3 (\mathcal{T} –21). Each point is an integration over 2 minutes of data. These variations are broad band (at least across the 300 MHz observing bandwidth) at 1.4 GHz. At higher frequencies, the pulsar is too weak to allow reliable flux densities to be obtained in a few minutes.

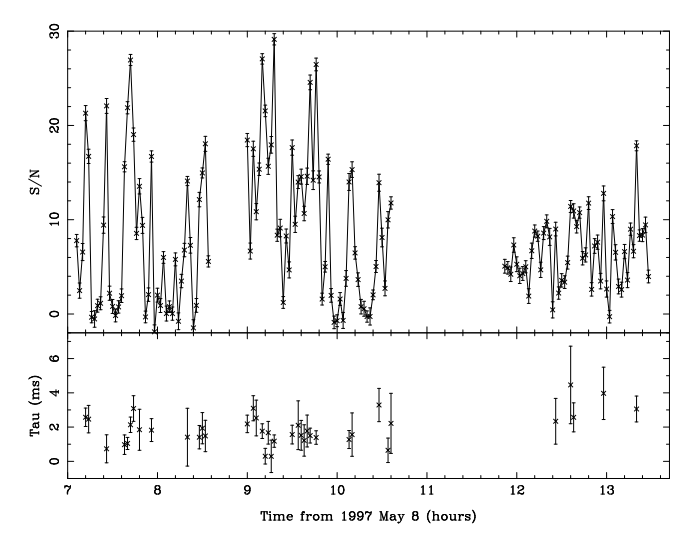


Figure 3. Top panel: Flux density of PSR B1259–63 on 1997 May 8. The observing frequency is 1.4 GHz and the fluctuations are broadband. Lower panel: Scattering time in ms for those integrations with large enough s/n to obtain reliable estimates.

This extreme flickering is only observed on \mathcal{T} –21. Observations made the previous day and on the following three days show only slow changes in flux density over hours and a much lower modulation index, consistent with the refractive scintillation timescale. \mathcal{T} –21 corresponds exactly to the first enhancement in the flux density seen in the unpulsed source (Johnston et al. 1999). This early increase in the flux density subsequently disappeared and does not fit well with the model of the unpulsed source (Ball et al. 1999), although Johnston et al. (1999) have argued that it is likely to be the result of the first interaction between the pulsar wind and the stellar disc coupled with optical depth effects.

4 DISCUSSION

At \mathcal{T} –20, the pulsar is ~50 stellar radii from the Be star. Assuming a wind density at the stellar surface of $7\times10^8\,\mathrm{cm}^{-3}$ which varies with radius as r^{-2} , the line-of-sight density to the pulsar should be ~3×10⁵ cm⁻³. However, one cannot expect this wind to be homogeneous and there are likely to be significant density variations because of turbulence.

We can use the equation derived by McClure-Griffiths et al. (1998) to relate the electron density in the scattering material, δn_e^2 , to the scattering parameters.

$$\delta n_e^2 = 4.0 \ \Delta \nu_{\rm d,MHz}^{-5/6} \ D_{\rm kpc}^{-5/6} \ \nu_{\rm GHz}^{11/3} \ \frac{l_{o,\rm pc}^{2/3}}{\Delta L_{\rm pc}} \ \left[\frac{(1+x)^2}{x} \right]^{5/6} \ {\rm cm}^{-6}(1)$$

Here, $\Delta\nu$ is the scintillation bandwidth, D the distance to the pulsar and ν the observing frequency. l_o is the outer scale length, ΔL is the thickness of the scattering screen and x is the ratio of the observer-screen distance and the pulsar-screen separation. We simplify this by using D=1.5 kpc, $\nu=1.4$ GHz and assuming $l_o\approx\Delta L$, $x\gg 1$ to obtain

$$\delta n_e^2 = 9.8 \quad \Delta \nu_{\rm d, MHz}^{-5/6} \quad x^{5/6} \quad \text{cm}^{-6}$$
 (2)

Converting the scintillation bandwidth, $\Delta\nu$ to the scattering time, τ , in milliseconds via $2\pi\tau\Delta\nu=1$ yields

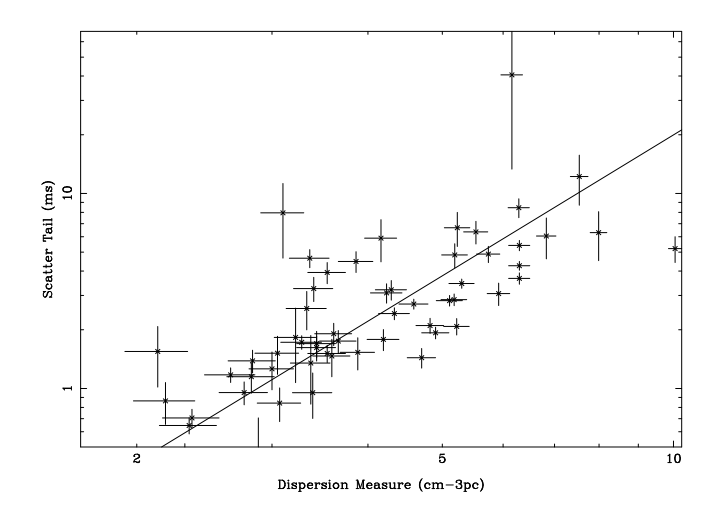


Figure 4. Scattering time versus change in DM at a given epoch. The straight line shows $\tau \propto \mathrm{DM}^{12/5}$.

$$\delta n_e^2 = 1.43 \times 10^4 \quad \tau^{5/6} \quad x^{5/6} \text{ cm}^{-6}$$
 (3)

Assuming a distance to the screen, r_s , of $\sim 8.4 \times 10^{12} \, \mathrm{cm}$, (i.e $x = 5.5 \times 10^8$), a scattering time of 3 ms gives δn_e^2 of $7 \times 10^{11} \, \mathrm{cm}^{-6}$ and hence n_e of $\sim 8.3 \times 10^5 \, \mathrm{cm}^{-3}$ assuming a fully modulated wind. This is remarkably close to the expected value obtained from a simple scaling of the electron density in the wind and shows that the scattering is caused by the global properties of the fully modulated wind. The size of the scattering disc, given by $(2\tau c r_s)^{1/2}$ is rather small, only 3.9×10^{10} cm.

These values are consistent with the DM measurements. A mean wind density of $\sim 8.3 \times 10^5 \, \mathrm{cm}^{-3}$ along a pathlength of roughly $2r_s$ yields a $\Delta \mathrm{DM}$ of 4.5 cm⁻³pc, close to the observed values. We also note that to double the observed scattering tail requires only a change in n_e of ~ 30 per cent and that this change affects the DM at the $\sim 1 \, \mathrm{cm}^{-3} \mathrm{pc}$ level. Such changes are seen on roughly a 2-hr timescale.

From equation 3 above it is evident that $\tau \propto n_e^{12/5}$ whereas DM $\propto n_e$. Providing the same electrons are responsible for the scattering and the dispersion we should observe that $\tau \propto {\rm DM}^{12/5}$. Figure 2 shows the expected correlation between dispersion measure and scattering time in that they both rise and fall together. In Figure 4 we show a plot of scattering time versus $\Delta {\rm DM}$. The scatter in the diagram leads to a large uncertainty in any formal straight line fit. For illustrative purposes, we show a line with slope 12/5 as derived above, which is in satisfactory agreement with the data.

Consider the free-free optical depth along the line of sight, given by

$$\tau_{\rm ff} = 8.2 \times 10^{-2} \ T^{-1.35} \ \nu^{-2.1} \int_0^d n_e^2 \ {\rm dl}$$
 (4)

where T is the temperature in Kelvin, ν the observing frequency in GHz, d the distance through the absorbing material in pc and n_e the free electron density within the clump. For an electron temperature in the wind of $\sim 10^4$ K (Waters 1986), the wind parameters described above yield $\tau_{\rm ff} \sim 0.6$ at 1.4 GHz, fully consistent with the lower flux densities recorded at these epochs. Flux density variations are seen both on timescales of a few minutes and on a roughly similar

timescale to the DM and scattering variations. The longer timescale is probably due to variations in the free-free optical depth, either because of temperature variations or small variations in the electron density. The short timescale variations generally have a low modulation index and are likely to be refractive scintillation. Given a timescale of $\sim\!200$ s for the variations and knowledge of the size of the scattering disc $(3.9\times10^{10}\,\mathrm{cm})$, the dominant velocity in the system is then $\sim\!2000~\mathrm{kms}^{-1}$. Such a velocity is consistent with UV observations of Be star winds in general.

In summary, we have shown that a plausible model for the wind of the Be star can account for the dispersion measure and scattering data before periastron and is also consistent with the variability timescale and the flux density variations. We stress that we are discussing the spherical, high-velocity, low-density wind from the star. The pulsar encounters the circumstellar disc material at \mathcal{T} –18, the density of the disc is so large that the pulsed flux becomes eclipsed shortly thereafter through a combination of free-free absorption and extreme pulse broadening and remains so until the pulsar re-emerges from the disc at \mathcal{T} +16. Post-periastron, the pulsar lies between the observer and the Be star. The path length through the stellar wind is much less than preperiastron and the DM and scattering variations are hence much smaller.

ACKNOWLEDGMENTS

We thank the Parkes staff, especially H. Fagg and M. Mc-Coll, for their considerable help throughout the observations. We thank M. Britton for useful discussions. The Australia Telescope is funded by the Commonwealth of Australia for operation as a National Facility managed by the CSIRO.

REFERENCES

Ball L. T., Melatos A., Johnston S., Skjaeraasen O., 1999, ApJ, 514, L39

Cominsky L., Roberts M., Johnston S., 1994, ApJ, 427, 978
Grove E., Tavani M., Purcell W. R., Kurfess J. D., Strickman M. S., Arons J., 1995, ApJ, 447, L113

Hirayama M., Nagase F., Tavani M., Kaspi V. M., Kawia N., Arons J., 1996, Proc. Astr. Soc. Jap., 48, 833

Hirayama M., Cominsky L. R., Kaspi V. M., Nagase f., Tavani M., Grove J. E., 1999, ApJ, 521, 718

Johnston S., Lyne A. G., Manchester R. N., Kniffen D. A.,
D'Amico N., Lim J., Ashworth M., 1992a, MNRAS, 255, 401
Johnston S., Manchester R. N., Lyne A. G., Bailes M.,
Kaspi V. M., Qiao G., D'Amico N., 1992b, ApJ, 387, L37

Johnston S., Manchester R. N., Lyne A. G., Nicastro L., Spyromilio J., 1994, MNRAS, 268, 430

Johnston S., Manchester R. N., Lyne A. G., D'Amico N., Bailes M., Gaensler B. M., Nicastro L., 1996, MNRAS, 279, 1026

Johnston S., Manchester R. N., McConnell D., Campbell-Wilson D., 1999, MNRAS, 302, 277

Kaspi V. M., Tavani M., Nagase F., Hirayama M., Hoshino M., Aoki T., Kawai N., Arons J., 1995, ApJ, 453, 424

King A., Cominsky L., 1994, ApJ, 435, 411

Manchester R. N., Johnston S., 1995, ApJ, 441, L65

McClure-Griffiths N., Johnston S., Stinebring D., Nicastro L., 1998, ApJ, 492, L49 Melatos A., Johnston S., Melrose D. B., 1995, MNRAS, 275, 381
Navarro J., 1994, PhD thesis, California Institute of Technology
Tavani M., Arons J., 1997, ApJ, 477, 439
Tavani M., Arons J., Kaspi V. M., 1994, ApJ, 433, L37
Waters L. B. F. M., 1986, AA, 162, 121
Wex N., Johnston S., Manchester R. N., Lyne A. G., Stappers B. W., Bailes M., 1998, MNRAS, 298, 997